PO Box 2345, Beijing 100023, China
www.wjgnet.com
wjg@wjgnet.com

ELSEVIER

World J Gastroenterol 2005;11(20):3070-3074
World Journal of Gastroenterology ISSN 1007-9327

• *BASIC RESEARCH* •

MR diffusion-weighted imaging of rabbit liver VX-2 tumor

You-Hong Yuan, En-Hua Xiao, Jun Xiang, Ke-Li Tang, Ke Jin, Shi-Jian Yi, Qiang Yin, Rong-Hua Yan, Zhong He, Quan-Liang Shang, Wei-Zhou Hu, Su-Wen Yuan

You-Hong Yuan, En-Hua Xiao, Jun Xiang, Ke-Li Tang, Ke Jin, Shi-Jian Yi, Qiang Yin, Rong-Hua Yan, Zhong He, Quan-Liang Shang, Wei-Zhou Hu, Su-Wen Yuan, Department of Radiology, the Second Xiangya Hospital, Central South University, Changsha 410011, Hunan Province, China
Supported by the National Natural Science Foundation of China, No. 30070235
Correspondence to: Dr En-Hua Xiao, Department of Radiology, the Second Xiangya Hospital, Central South University, Changsha 410011, Hunan Province, China. xiaogdk@sohu.com
Telephone: +86-731-5550355 Fax: +86-731-4510190
Received: 2004-05-27 Accepted: 2004-06-17

Abstract

AIM: To investigate the implanting method of rabbit liver VX-2 tumor and its MR diffusion-weighted imaging (DWI) characteristics.

METHODS: Thirty-five New Zealand rabbits were included in the study. VX-2 tumor was implanted subcutaneously in 14 rabbits and intrahepatically in 6 for pre-experiments. VX-2 tumor was implanted intrahepatically in 12 rabbits for experiment and three were used as the control group. DWI, T1- and T2-weighted of MRI were performed periodically in 15 rabbits for experiment before and after implantation. The distinction of VX-2 tumors on DWI was assessed by their apparent diffusion coefficient (ADC) values. The statistical significance was calculated by analysis of variance (ANOVA) of the randomized block design using SPSS10.0 software.

RESULTS: The successful rate of subcutaneous implantation of VX-2 tumor was 29% (4/14) while that of intrahepatic implantation of it was 33% (2/6) in the preexperiment. The successful rate of intrahepatic implantation of VX-2 tumor in the experiment was 83% (10/12) and 15 tumors grew in 10 successfully implanted rabbits. The DWI signal of VX-2 tumor was high and became lower when the *b* value increased step by step. The signal of VX-2 tumor on the map of ADC was low. When the *b* value was 100 or 300 s/mm^2, the ADC value of normal group and VX-2 tumor group was respectively 2.57±0.26, 1.73±0.31, 1.87±0.25 and 1.57±0.23 mm^2/s. Their distinction was significant (F = 43.26, P<0.01), the tumor ADC value between *b* values 100 and 300 s/mm^2 was significant (Tukey HSP, P<0.05) and the ADC value between VX-2 tumor and normal liver was also significant (Tukey HSP, P<0.01). VX-2 tumor developed quickly and metastasized early to all body, especially to the lung, liver, lymph nodes of mediastinum, *etc*.

CONCLUSION: The DWI signal of rabbit VX-2 tumor has its characteristics on MR DWI and DWI plays an important role in diagnosing and discovering VX-2 tumor.

Key words: Magnetic resonance imaging; Diffusion-weighted; Liver; VX-2 tumor; Rabbits

Yuan YH, Xiao EH, Xiang J, Tang KL, Jin K, Yi SJ, Yin Q, Yan RH, He Z, Shang QL, Hu WZ, Yuan SW. MR diffusion-weighted imaging of rabbit liver VX-2 tumor. *World J Gastroenterol* 2005; 11(20): 3070-3074
http://www.wjgnet.com/1007-9327/11/3070.asp

INTRODUCTION

The main imaging diagnostic methods of hepatic tumor include computed tomography (CT), magnetic resonance imaging (MRI) and ultrasonography (US)[1-4]. In recent years, however, the application of MRI, especially MR diffusion-weighted imaging (DWI) in the diagnosis of hepatic tumor and evaluation of its progression is much less than that of CT and US[5-8]. With the development of software and scanning technology of MRI, many problems, for example, poor imaging quality, slow scanning speed, have been overcome[8-11] and more studies on it have been reported in recent years[12-15].

Diffusion is caused by the free movement of water molecule[8,10,13-16]. The amount of diffusion is determined by the diffusion coefficient (DC). However, because the measurement of DC *in vivo* may be affected by many factors, such as temperature, perfusion, magnetic susceptibility in the tissue, or other kinds of the motion, the apparent diffusion coefficient (ADC) is used much more in clinic than DC[14,17-19]. DWI was initially used to evaluate early ischemic stages of the brain and its values have been accepted in recent years all over the world. At the same time, several research groups have concluded that DWI has great potential for understanding normal and pathological brain function[20]. But few studies are available on the value of DWI in diagnosing or evaluating the progression of hepatic lesions, especially the VX-2 tumor of rabbits[17,21-23].

Hepatocellular carcinoma (HCC) is one of the most frequent tumors and many studies about its CT, DSA, MRI characteristics have been undertaken in recent years[3-5,6-9,24]. Rabbit VX-2 tumor is the most valuable animal model of HCC in researching its imaging characteristics[25,26], because the blood supply to VX-2 tumor and HCC is similar[23,26,27].

The purpose of our experiment was to investigate the

implanting method of rabbit liver VX-2 tumor and the characteristics of rabbit VX-2 tumor on DWI.

MATERIALS AND METHODS

Animals

Animal studies were carried out under the supervision of a veterinarian according to the guidelines of Ministry of Public Health of China for the use of laboratory animals. All animals were provided by the Laboratory Animal Center of the Second Xiangya Hospital and all protocols were approved by the Animal Use and Care Committee of the Second Xiangya Hospital.

Establishment of VX-2 tumor model[17-20]

The VX-2 tumor strain of rabbit was provided by the Fourth Military Medical University.

Our experiment was divided into two steps: pre-experiment during which subcutaneous and intrahepatic implantation of VX-2 tumor was carried out; experiment during which VX-2 tumor cells were harvested and implanted into the rabbit liver after they grew up under the rabbit derm. Ten of the twenty New Zealand white rabbits in preexperiment were male and 10 were female, their weight ranged from 1.5 kg to 2.0 kg. Six had intrahepatic implantation while 14 had subcutaneous implantation. Eight of the 15 New Zealand white rabbits in the experiment were male and seven were female, their weight ranged from 2.0 to 3.0 kg. Twelve had intrahepatic implantation while the others served as controls.

Procedure of implantation[19-23]

First, we extracted the VX-2 tumor strain from the subcutaneous tumor which was implanted during the preexperiment. After the rabbits were anesthetized, by injecting 3% soluble pentobarbitone into auriborder vein or abdominal cavity at a dose of 1 mL/kg, we incised the skin to expose one cauliflower of the tumor and then excised one cauliflower from it. Then we put the tumor parenchyma into saline containing 40 000 unit gentamycin per 100 mL, and discarded the necrosed tissue and blood clot and then cut it into 1-2 mm^3 microblocks.

Second, we implanted the VX-2 tumor strain into the subcutaneous or liver parenchyma. During the subcutaneous implanting, we pushed the VX-2 tumor strain into the subcutaneous connective tissue through the implanting tube after disinfecting and excising the skin. As the liver parenchyma implanting was concerned, we exposed the lobe of liver after excising the skin and vagina musculi recti abdominis. We put the implanting tube containing the VX-2 tumor strain into the chosen-lobe by rotating and push the VX-2 tumor strain into the liver parenchyma, then put the gelatin sponge into the implanting stoma to prevent bleeding. After the liver stopped bleeding, we sutured the peritoneum, musculi, and skin, respectively. Six of the fifteen New Zealand white rabbits in experiment were implanted in one lobe while six were implanted in two lobes.

After implanting, we injected 200 000-unit penicillin into the muscle daily for 4 d. At the same time, the animal room was kept dry and ventilated.

Magnetic resonance imaging protocol[19]

After animals were anesthetized by injecting 3% soluble pentobarbitone into auriborder vein at a dose of 1 mL/kg or at different doses based on different animal status to make sure that the breathing of animals was slow and stable, T1WI, T2WI, and DWI were performed on a 1.5-Tesla Sigma Twinspeed MR scanner (General Electron Medical Systems, USA) using a small diameter cylindrical brain radiofrequency coil. DWI (axial) and MRI (T1WI and T2WI, axial and coronal) were obtained respectively and periodically 1 d before implanting and 7, 14, 21, or 35 d after implant. The scanning parameters of DWI included spin echo echoplanar imaging (SE-EPI) series, *b*-values 100 and 300 s/mm^2, repetition time (TR) 6 000 ms, echo time (TE) 45 ms, 20 cm×15 cm field of view (FOV), 8NEX, 2 mm thickness layer, 0.5 mm Space, 128×128 matrix, *etc*. The scanning parameters of common MRI included fast reverse fast spin echo (FRFSE) series, T1WI (TR 400/TE 12.3 ms), T2WI (TR3000/TE80 ms), 20 cm×15 cm FOV, 4 NEX, 5 mm thick layer, 0 mm space, 256×192 (T1WI) and 320×256 (T2WI) matrix, *etc*.

Statistical analysis

Based on apparent diffusion coefficient (ADC) value of regions of interest (ROIs), images were evaluated quantitatively, including the difference between normal rabbit liver parenchyma and VX-2 tumor and between different *b*-value groups. ADC values of normal rabbit parenchyma were obtained by the average value of five different ROIs (50 mm^2 each area). We took 80% rabbit VX-2 tumor area as their ROI and measured their ADC values.

The statistical significance was calculated by analysis of variance (ANOVA) of the randomized block using SPSS10.0 software.

RESULTS

Results of rabbit VX-2 tumor implantation

The results of rabbit VX-2 tumor implantation are shown in Table 1.

Table 1 Results of rabbit VX-2 tumor implant

Methods	Number	Success of implant	Postoperative infection	Postoperative death	Cause of death	Rate of success (%)
Pre-experiment						
Intraderm	14	4	0	4	Diarrhea	29 (4/14)
Intrahepatic	6	2	0	2	Diarrhea	33 (2/6)
Experiment						
Intrahepatic	12	10	0	1	Diarrhea	83 (10/12)

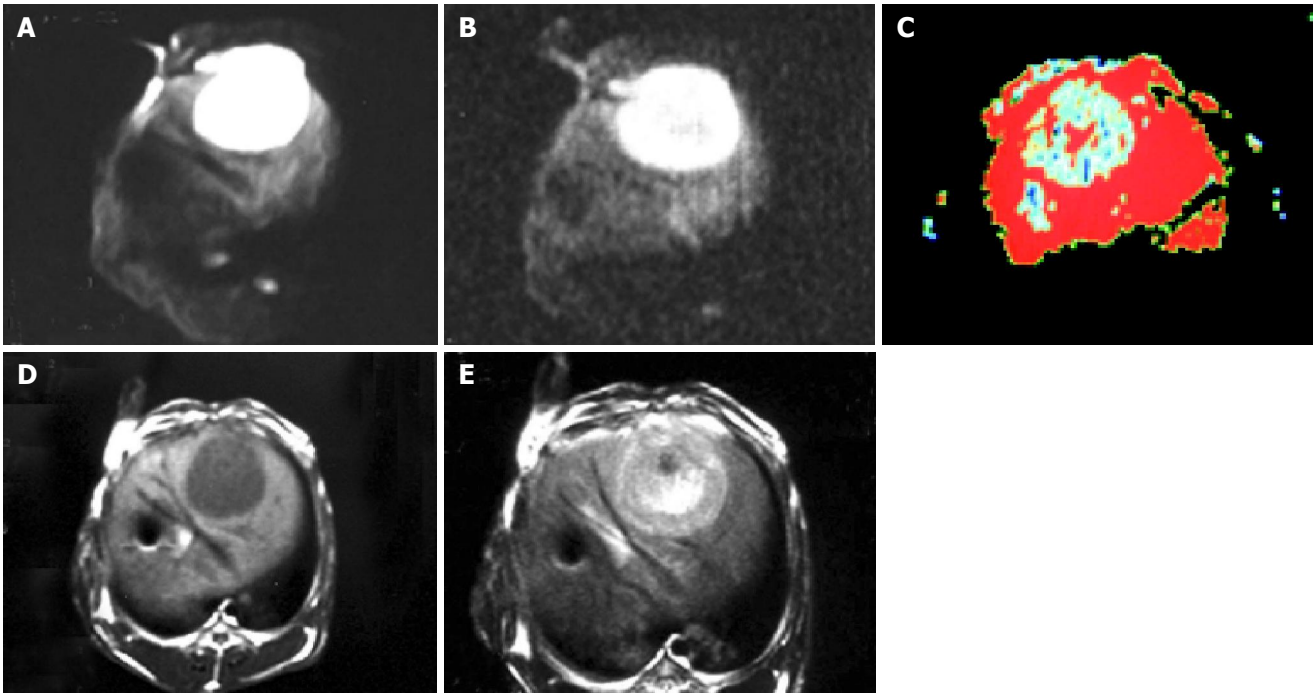

Figure 1 Image manifestations of hepatic VX-2 tumor on DWI. **A**: High signal and distinct, sharp margin of VX-2 tumor on DWI when *b* value is 100; **B**: High signal and distinct margin of VX-2 tumor on DWI when *b* value was 300; **C**: Blue-green VX-2 tumor and red normal liver parenchyma when *b* value was 100; **D**: Low signals and distinct margin of VX-2 tumor on T1WI (note: the no signal area in liver is artifact); **E**: Slightly high signals and distinct margin of VX-2 tumor on T2WI (note: the low signal in the middle of the tumor is gelatin sponge and the no signal area in liver is artifact).

Image manifestations of hepatic VX-2 tumor

Fifteen tumors were detected in 10 rabbit hepatic parenchymas. The diameter of the tumor was 4.73±0.78 on d 7, 11.35±1.73 on d 14, 21.82±3.12 on d 21, and 43.25±4.32 on d 35.

The image quality and tumor signal of DWI were higher when the *b*-value was 100 than those when the *b*-value was 300 (Figures 1A and B). Eight tumors were detected with *b*-value 100 on DWI while 10 tumors were detected with *b*-value 300 on the 7th d after implantation and 15 tumors were detected on DWI with *b*-value 100 or 300 after 14 d. All tumors showed high signals on DWI. The tumor signal on DWI was fairly uniform 14 d after implantation while it was not uniform on the 21th and 35th d and it also showed higher signals in different area tumor sometimes. In addition, one or two low signal areas could be seen in three tumors on the 21th d. T1WI, T2WI or DWI could not be seen on d 35. The margin of 15 tumors not only displayed distinctly but also differed significantly from the structure around. ADC values of all tumors are summarized in Table 2. As shown in Figure 1C, 12 of the 15 cases appeared to have low signals while three were equal or slightly low signals. The number of displayed tumors on T1WI and T2WI was same as that on DWI on the 21th or 35th d. The tumors displayed low signals on T1WI and high signals on T2WI. In addition, the margin of most tumors was distinct but less significant on T1WI or T2WI (Figures 1D and E) between the tumor and the liver parenchyma with different than that on DWI (Figures 1A and B). One of them displayed multi-tumors sizes, the biggest diameter of tumor was about 4 cm×4 cm. They showed different high signals on DWI, and low signals on TIWI and high signals on T2WI. In addition, the size of low signal zones was different in the tumor. The results of autopsy are shown in Figure 2.

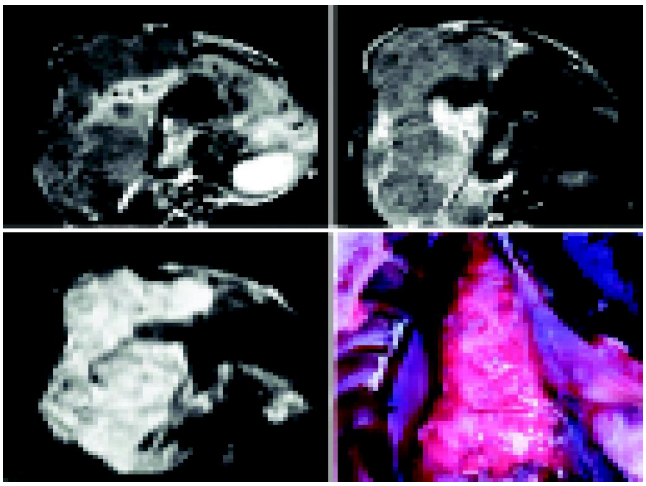

Figure 2 Pleural effusion, abdominal cavity fluid, multi-metastases in the lungs and lymph nodes 21 d after implantation of VX-2 tumor.

Table 2 ADC values of normal rabbit liver and VX-2 tumor (mean±SD)

	ADC values	A[1]	B[1]	C[1]	D[1]	*F*	*P*
A[1]	2.57±0.26		*P*<0.01[2]	*P*<0.01[2]	*P*<0.01[2]		
B[1]	1.73±0.31	*P*<0.01					
C[1]	1.87±0.25	*P*<0.01			*P*<0.05[2]		
D[1]	1.57±0.23	*P*<0.01		*P*<0.05[2]			
ANOVA						43.26	*P*<0.01

[1]A – normal rabbit liver DWI (b = 100 s/mm^2); B – normal rabbit liver DWI (b = 300 s/mm^2); C – VX-2 tumor DWI (b=100 s/mm^2); D – VX-2 tumor DWI b=100 s/mm^2); [2]Difference between different *b*-value groups or between normal liver parenchyma group and VX-2 tumor group.

Table 3 Progression of intrahepatically implanted VX-2 tumor in 12 rabbits

No.	Common conditions[1]						Transferring conditions[2] (MRI and autopsy)								Survival time (d)
	7 d	14 d	21 d	28 d	35 d	40 d	A	B	C	D	E	F	G	H[3]	
1	1	1	2	4			+	+	+	–	–	–	–	–	28
2	1	1	2	3	3	3	–	+	–	–	+	–	–	–	>40
3	1	1	3	3	3	4	+	+	+	–	–	+	+	–	39
4	4						–	–	–	–	–	–	–	–	3
5	1	1	1	1	1	1	–	–	–	–	–	–	–	–	>40
6	2	1	2	3	3	3	+	+	+	–	+	+	–	–	>40
7	1	1	1	3	4		–	+	–	–	–	–	+	–	33
8	3	2	3	3	3	3	+	+	+	–	+	–	–	–	>40
9	1	1	2	3	3	4	+	+	+	–	+	–	+	–	38
10	1	1	2	3	4		–	+	+	–	–	–	+	–	32
11	1	2	3	3	3	3	–	+	–	–	+	–	–	–	>40
12	1	1	3	3	3	4	+	+	+	–	+	–	+	–	39

[1]Common conditions: 1 – well; 2 – common; 3 – bad; 4 – dead. [2]Transferring or metastasizing conditions:– no transferring or metastasizing; + transferring or metastasizing. [3]A – liver; B – lung; C – mediastina; D – brain; E – thoracic or abdominal cavity; F – postperitone; G – diaphragm and heart; H – kidney or pancreas.

Progressing and transferring of rabbit liver VX-2 tumor

MRI and DWI were performed periodically on 12 rabbits in experiment to observe their growing and transferring or metastasizing characteristics (Table 3).

Manifestations of VX-2 tumor dissection and pathology

Intrahepatic VX-2 tumor appeared pale with no envelope and identifiable margin, the extrahepatic surface was uneven (Figure 3). Lung metastases showed many pale nodular foci in size of Mung bean or soybean (Figure 2). After the tumor was removed, the extralayer was thick and tough with rich blood supply. The interior tumor cells were pale. When the tumor grew bigger, irregular cavities could be found in it. Under low power microscope, we could see multilump nests without clear margin. In addition, more parenchyma tissue was found in the tumor than connective tissue in the tumor and there were rich and new blood capillaries between tumor cells. Calcified part in VX-2 tumors could be observed at times. Under high power microscope, VX-2 tumor cells mainly were big and irregular. In addition, the cytoplasm was rich and the nuclei were thickly stained and irregular.

Figure 3 Pale nodular foci of VX-2 tumor 14 d after implanting.

DISCUSSION

VX-2 tumor is induced by the Shope virus and develops after 72 times or more transfer of culture[17,23,24]. Its blood is mainly supplied by the hepatic artery. VX-2 tumor is implanted easily and grows quickly so that the diameter of the tumor can reach 2 cm, 3 or more weeks after implanted and it is able to metastasize to the liver, the lung, mediastinum in the early stage, which is suitable for making animal models. The rate of lung metastasis was 91% (10/11) in our group. In addition, it is advantageous to be manifested by imaging because VX-2 tumor is a solid tumor and rabbit weight is relatively great. Thus, in research of HCC imaging, VX-2 tumor is the widely used animal model[24,25].

The methods of VX-2 tumor implantation mainly include tumor cell injection by hepatic artery catheterization, percutaneous transhepatic injection of tumor cells and direct intrahepatic tumor block implantation[23,24,27]. The successful rate of the last method is the highest, which is usually more than 90%, while that of other two methods is relatively low, which is often lower than 70%[24-26]. In our experiment, we chose tumor block implanting and found the successful rate of intrahepatic implantation was 83% in experiment and 33% in pre-experiment and that of subcutaneous implantation was 29%. For this, on the one hand, we have not gotten the most vigorous tumor cells because of our poor experience and, on the other hand, many rabbits die of diarrhea because of dampness and poorly ventilated animal room as well as rabbits of unsuitable weight and age. In order to increase the successful rate, it is very important to pay attention to these implant technologies. First, we should get the most vigorous tumor cells, the mother of which is no more than 21 d after being implanted and which is observed to be pale or resembling fish flesh and is easy to separate from the tumor. Second, we should choose an appropriate implanting spot, reduce bleeding and prevent abdominal cavity implantation. Finally, clean, ventilated, dry living environment and healthy, strong rabbits are also very important.

Diffusion is caused by the free movement of water molecule, known as "Brown motion". It is able to change the intensity of local magnetic field around hydrogen proton so that its phase position in magnetic field is changed. If we add a powerful polar and quick switching gradient

radiofrequent (RF) pulse, we are able to amplify these phase changes so that we can detect water molecule diffusion motion, known as diffusion-weighted imaging (DWI). The signals on DWI are low when water molecule diffusion motion is high while the signals on DWI are high when water molecule diffusion motion is low. VX-2 tumor is a solid tumor and its body mainly consists of tumor cell nests and other cells so that its water molecule diffusion motion is restricted. The signals of most VX-2 tumor on DWI are high and its margin is usually distinct (Figures 1A and B). When *b* value increases, the signals of VX-2 tumor become lower and lower (Figures 1A and B) but the ability to detect lesions becomes stronger and stronger. All the 15 VX-2 tumors showed high signals in our experiment and the signals of tumors were lower when *b* value was 300 than when it was 100 (Figures 1A and B). The amount of diffusion is determined by the diffusion coefficient (DC). Because DC is affected by many factors, the apparent diffusion coefficient (ADC) is used more clinically rather than DC. In our experiment, the mean ADC value of 15 VX-2 tumors was 1.87±0.25 while that of the normal hepatic parenchyma was 2.57±0.26. When *b* value increased, ADC value became low. The mean ADC value of VX-2 tumor was 1.87±0.25 when *b* value was 100 while it was 1.57±0.23 when *b* value was 300.

In conclusion, the hepatic VX-2 tumor model is a simple and efficient HCC model. DWI has potentially important value in reflecting water molecular motion of tumor, detecting tumor and monitoring tumor progression.

ACKNOWLEDGMENTS

We thank the staff of the Radiology Department and the Laboratory Animal Center of the Second Xiangya Hospital for their help and support, especially Miss Ying-Si He.

REFERENCES

1 **Blomqvist L.** Preoperative staging of colorectal cancer-computed tomography and magnetic resonance imaging. *Scand J Surg* 2003; **92**: 35-43
2 **Vilana R,** Llovet JM, Bianchi L, Sanchez M, Pages M, Sala M, Gilabert R, Nicolau C, Garcia A, Ayuso C, Bruix J, Bru C. Contrast-enhanced power Doppler sonography and helical computed tomography for assessment of vascularity of small hepatocellular carcinomas before and after percutaneous ablation. *J Clin Ultrasound* 2003; **31**: 119-128
3 **Braga L,** Guller U, Semelka RC. Modern hepatic imaging. *Surg Clin North Am* 2004; **84**: 375-400
4 **Vogl TJ,** Schwarz W, Blume S, Pietsch M, Shamsi K, Franz M, Lobeck H, Balzer T, del Tredici K, Neuhaus P, Felix R, Hammerstingl RM. Preoperative evaluation of malignant liver tumors: comparison of unenhanced and SPIO (Resovist)-enhanced MR imaging with biphasic CTAP and intraoperative US. *Eur Radiol* 2003; **13**: 262-272
5 **Taouli B,** Vilgrain V, Dumont E, Daire JL, Fan B, Menu Y. Evaluation of liver diffusion isotropy and characterization of focal hepatic lesions with two single-shot echo-planar MR imaging sequences: prospective study in 66 patients. *Radiology* 2003; **226**: 71-78
6 **Ichikawa T,** Araki T. Fast magnetic resonance imaging of liver. *Eur J Radiol* 1999; **29**: 186-210
7 **Harvey PR.** The modular (twin) gradient coil-high resolution, high contrast, diffusion weighted EPI at 1.0 Tesla. *MAGMA* 1999; **8**: 43-47
8 **Stahlberg F,** Brockstedt S, Thomsen C, Wirestam R. Single-shot diffusion-weighted echo-planar imaging of normal and cirrhotic livers using a phased-array multicoil. *Acta Radiol* 1999; **40**: 339
9 **Ferrucci JT.** Advances in abdominal MR imaging. *Radiographics* 1998; **18**: 1569-1586
10 **Yamashita Y,** Tang Y, Takahashi M. Ultrafast MR imaging of the abdomen: echo planar imaging and diffusion-weighted imaging. *J Magn Reson Imaging* 1998; **8**: 367-374
11 **Chow LC,** Bammer R, Moseley ME, Sommer FG. Single breath-hold diffusion-weighted imaging of the abdomen. *J Magn Reson Imaging* 2003; **18**: 377-382
12 **Colagrande S,** Politi LS, Messerini L, Mascalchi M, Villari N. Solitary necrotic nodule of the liver: imaging and correlation with pathologic features. *Abdom Imaging* 2003; **28**: 41-44
13 **Murtz P,** Flacke S, Traber F, van den Brink JS, Gieseke J, Schild HH. Abdomen: diffusion-weighted MR imaging with pulse-triggered single-shot sequences. *Radiology* 2002; **224**: 258-264
14 **Amano Y,** Kumazaki T, Ishihara M. Single-shot diffusion-weighted echo-planar imaging of normal and cirrhotic livers using a phased-array multicoil. *Acta Radiol* 1998; **39**: 440-442
15 **Kim T,** Murakami T, Takahashi S, Hori M, Tsuda K, Nakamura H. Diffusion-weighted single-shot echoplanar MR imaging for liver disease. *AJR Am J Roentgenol* 1999; **173**: 393-398
16 **Kamel IR,** Bluemke DA, Ramsey D, Abusedera M, Torbenson M, Eng J, Szarf G, Geschwind JF. Role of diffusion-weighted imaging in estimating tumor necrosis after chemoembolization of hepatocellular carcinoma. *AJR Am J Roentgenol* 2003; **181**: 708-710
17 **Ichikawa T,** Haradome H, Hachiya J, Nitatori T, Araki T. Diffusion-weighted MR imaging with single-shot echo-planar imaging in the upper abdomen: preliminary clinical experience in 61 patients. *Abdom Imaging* 1999; **24**: 456-461
18 **Moteki T,** Horikoshi H, Oya N, Aoki J, Endo K. Evaluation of hepatic lesions and hepatic parenchyma using diffusion-weighted reordered turboFLASH magnetic resonance images. *J Magn Reson Imaging* 2002; **15**: 564-572
19 **Chan JH,** Tsui EY, Luk SH, Fung AS, Yuen MK, Szeto ML, Cheung YK, Wong KP. Diffusion-weighted MR imaging of the liver: distinguishing hepatic abscess from cystic or necrotic tumor. *Abdom Imaging* 2001; **26**: 161-165
20 **Lodi R,** Tonon C, Stracciari A, Weiger M, Camaggi V, Iotti S, Donati G, Guarino M, Bolondi L, Barbiroli B. Diffusion MRI shows increased water apparent diffusion coefficient in the brains of cirrhotics. *Neurology* 2004; **62**: 762-766
21 **Ichikawa T,** Haradome H, Hachiya J, Nitatori T, Araki T. Diffusion-weighted MR imaging with a single-shot echoplanar sequence: detection and characterization of focal hepatic lesions. *AJR Am J Roentgenol* 1998; **170**: 397-402
22 **Yuan YH,** Xiao EH. MR diffusion-weighted imaging progressing in liver. *J Practice Radiology* 2003; **19**: 945-948
23 **Geschwind JF,** Artemov D, Abraham S, Omdal D, Huncharek MS, McGee C, Arepally A, Lambert D, Venbrux AC, Lund GB. Chemoembolization of liver tumor in a rabbit model: assessment of tumor cell death with diffusion-weighted MR imaging and histologic analysis. *J Vasc Interv Radiol* 2000; **11**: 1245-1255
24 **Jia HS,** Quan XY, Zeng S, Wen ZB. Dynamic evaluation of rabbit VX2 hepatic carcinoma with CT and MRI. *Diyi Junyi Daxue Xuebao* 2002; **22**: 141-144
25 **Minami Y,** Kudo M, Kawasaki T, Kitano M, Chung H, Maekawa K, Shiozaki H. Transcatheter arterial chemoembolization of hepatocellular carcinoma: usefulness of coded phase-inversion harmonic sonography. *AJR Am J Roentgenol* 2003; **180**: 703-708
26 **Kuszyk BS,** Boitnott JK, Choti MA, Bluemke DA, Sheth S, Magee CA, Horton KM, Eng J, Fishman EK. Local tumor recurrence following hepatic cryoablation: radiologic-histopathologic correlation in a rabbit model. *Radiology* 2000; **217**: 477-486
27 **Merkle EM,** Boll DT, Boaz T, Duerk JL, Chung YC, Jacobs GH, Varnes ME, Lewin JS. MRI-guided radiofrequency thermal ablation of implanted VX2 liver tumors in a rabbit model: demonstration of feasibility at 0.2 T. *Magn Reson Med* 1999; **42**: 141-149

Science Editor Wang XL **Language Editor** Elsevier HK